Author Manuscript

Author Manuscript

Author Manuscript

Author Manuscript

HHS Public Access

Author manuscript

Neurosci Lett. Author manuscript; available in PMC 2017 January 01.

Published in final edited form as:

Neurosci Lett. 2016 January 1; 610: 110–116. doi:10.1016/j.neulet.2015.10.066.

A close look at axonal transport: cargos slow down when crossing stationary organelles

Daphne L. Che, **Praveen D. Chowdary**, and **Bianxiao Cui**

Department of Chemistry, Stanford University, Stanford, CA 94305

Abstract

The bidirectional transport of cargos along the thin axon is fundamental for the structure, function and survival of neurons. Defective axonal transport has been linked to the mechanism of neurodegenerative diseases. In this paper, we study the effect of the local axonal environment to cargo transport behavior in neurons. Using dual-color fluorescence imaging in microfluidic neuronal devices, we quantify the transport dynamics of cargos when crossing stationary organelles such as non-moving endosomes and stationary mitochondria in the axon. We show that the axonal cargos tend to slow down, or pause transiently within the vicinity of stationary organelles. The slow-down effect is observed in both retrograde and anterograde transport directions of three different cargos (TrkA, lysosomes and TrkB). Our results agree with the hypothesis that bulky axonal structures can pose as steric hindrance for axonal transport. However, the results do not rule out the possibility that cellular mechanisms causing stationary organelles are also responsible for the delay in moving cargos at the same locations.

Keywords

fluorescence imaging; transport dynamics; roadblocks; axonal swelling; pseudo-TIRF microscopy; axonal transport

INTRODUCTION

Neurons have extensive axons that span up to 10,000 times the length of their cell bodies. Despite their great length, axons have very little protein synthesis capacity; therefore neurons must rely on axonal transport, the bidirectional traffic of materials along the axon, for proper growth, maintenance, and functioning [1]. Disruption in this process could lead to dreadful consequences such as neurodegenerative diseases [2]. Axonal swellings with aberrant local accumulation of axonal cargos are the common marker of the pathogenesis. In human Alzheimer's disease (AD) brain and a mouse AD model, abnormal axonal swellings were found to precede amyloid formation and other disease-related pathology by at least one year [3]. Significant deficit in retrograde transport was also observed in presymptomatic amyotrophic lateral sclerosis mice model [4]. These reports have supported the hypothesis

Publisher's Disclaimer: This is a PDF file of an unedited manuscript that has been accepted for publication. As a service to our customers we are providing this early version of the manuscript. The manuscript will undergo copyediting, typesetting, and review of the resulting proof before it is published in its final citable form. Please note that during the production process errors may be discovered which could affect the content, and all legal disclaimers that apply to the journal pertain.

Author Manuscript Author Manuscript Author Manuscript Author Manuscript

that defective axonal transport may be a key event, or even the cause, in the development of neurodegenerative diseases.

Nevertheless, the mechanism causing axonal transport deficits is still not well understood. Axonal transport malfunctions can be directly caused by defects in the transport machinery such as mutations in motor proteins or cargo adaptor proteins [5]. For example, Loa and Cra1 transgenic mouse models featuring point mutations in the heavy chain of the molecular motor dynein have been found to display defective retrograde transport and progressive motor neurons degeneration [6]. Deficits in axonal transport can also be caused by unfavorable axonal environment such as frequent breaks in microtubule tracks or congested traffic conditions caused by local organelle accumulation.

Previous studies of intracellular trafficking of cargos in cell lines have suggested that the local cytoskeletal and organelle interactions can strongly affect cargo motility, causing pauses at the point of interaction [7, 8]. Earlier reports showed that drug-induced mitochondrial swelling led to a decrease in the average axonal transport speed of mitochondria and lysosomes, suggesting that an increase in mitochondrial size causes steric hindrance for axonal transport [9, 10]. However, in these studies, mitochondrial swelling was coupled with the loss of mitochondrial membrane potential, and it is still debatable whether the impaired axonal transport was a result of congested traffic condition, or it was because the ATP production activity of mitochondria had been compromised.

Here we examine the impact of local axonal environment on the transport of axonal cargos without drug perturbation. Axonal sites with stationary organelles, either with non-moving organelles or stationary mitochondria, are marked as sites of interests and we examine whether and how moving cargos exhibit different dynamics at these locations. Our results demonstrate that moving cargos are prone to slow down when crossing stationary organelles. Both the retrogradely and the anterogradely moving cargos show similar behavior. Quantitative analysis shows that the moving cargos are more likely to exhibit transient pauses when crossing stationary organelles. While in healthy neurons these sites of interests only cause a mild delay in the transport of the axonal cargos, they may play a more important role in causing transport deficit in disease conditions.

MATERIALS AND METHODS

Primary neuronal cell culture

Dorsal root ganglion (DRG) neurons were isolated from E18 Sprague Dawley rat embryos and maintained in neurobasal medium supplemented with B27, 2 mM glutamax, and 50 ng/ml NGF according to a published protocol [11]. Media and reagents were obtained from Invitrogen (Carlsbad, CA).DRG cells were transiently transfected using Nucleofector method (Lonza, Switzerland) before plated in microfluidic devices. The devices used in this study featured two individual chambers connected by a set of micron-size channels [12]. This design allowed the separation of cell bodies and axonal terminals, thus making it straight forward to differentiate the direction of axonal transport, i.e. anterograde vs. retrograde direction. For single-color transport experiments, the cells were transfected with TrkA-mCherry. For dual-color transport experiments, the cells were co-transfected with

Author Manuscript Author Manuscript Author Manuscript Author Manuscript

either TrkA-mCherry and Mito-YFP or LAMP1-mCherry and Mito-YFP. Cytosine arabinoside (4 μM) was added 24 h after plating to reduce glial cell growth. The cultures were housed in a humidified incubator with 5% CO_2 at 37°C for 6–7 days before imaging. On day 7 *in vitro*, the culture medium was switched to CO_2-independent medium (Life Technologies, Carlsbad, CA) for live-cell imaging. For experiments with hippocampal neurons, E18 rat hippocampi were dissociated and maintained similarly to the DRG protocol. Hippocampal neurons were co-transfected with Mito-YFP and TrkB-mCherry using Lipofectamine 2000 (Life Technologies, Carlsbad, CA) on day 4 *in vitro* and imaged on day 7 *in vitro*.

Live imaging of cargo axonal transport using pseudo-TIRF microscopy

Fluorescence imaging of cargo transport was carried out using a homebuilt pseudo total internal reflection fluorescence (pseudo-TIRF) microscope as previously described [12]. Briefly, the incident angle of the excitation laser was adjusted to be slightly smaller than the critical angle so that the laser beam could penetrate approximately 1–3μm deep into the sample (a depth comparable to the diameter of DRG axons). A homemade on-stage temperature control system maintained the temperature of the imaging culture to be 37°C. To enable simultaneous observation of different cargos inside the neuron (i.e., mitochondria vs. TrkA or mitochondria vs. lysosomes), two lasers, 488 nm and 561 nm (Spectra-Physics, Santa Clara, CA), were used to excite yellow fluorescence protein (YFP) and a variant of red fluorescence protein (mCherry), respectively. The fluorescence emission was collected by a 100× TIRF objective (Nikon, NA 1.49) and was split by a 550 nm dichroic mirror. The two spectrally resolved emission signals were further filtered by passing through a 520/40 or a 605/20 emission filter. The two images were then separated onto two halves of a back illuminated EMCCD camera (Andor iXon DU-897E) (Fig.1A). Movies were taken for 500–1000 frames at 10Hz frame rate.

Data analysis using custom-written Matlab program

There are three main steps in data analysis: kymograph generation, trajectory tracing, and transport behavioral quantification (Fig. 1A–B and Fig. S1). The spatiotemporal kymograph of the transporting cargos in the axon was generated as detailed in a previous publication [13]. Briefly, as the cargos travel along the axon, their fluorescent intensities map out the shape of the axon (Fig.S1A–B). A kymograph of the moving cargos was constructed by plotting the fluorescence intensity profile along the axonal shape over the duration of the movie (Fig.S1C).

From the kymograph, we quantified cargo transport behavior when crossing the stationary markers. The moving cargo trajectories were traced using a custom written Matlab program (Fig. 1B, red dots). The data is further separated into two transport directions, i.e. retrograde vs. anterograde. The positions of the stationary organelles, either non-moving TrkA or stationary mitochondria, were traced separately (Fig. 1B, white traces). For single-color TrkA transport experiments, the width of the non-moving TrkA markers was fixed at 1.5μm (9 pixels) (Fig. 1B). For dual-color transport experiments, the width of each stationary mitochondrial site varied depending on the length of mitochondrial fluorescent signals (Fig. 2A and Fig. S3). The Matlab program automatically identified the crossing events of the

Author Manuscript Author Manuscript Author Manuscript Author Manuscript

moving cargos and the stationary markers in the kymograph. At each crossing event, the cargo's average speed within the stationary site (v_{inside}) and its average speed in the region immediately before the site (v_{before}) can be calculated (length of the region divided by the time it takes for the cargo to cross the specified region) (Fig. 1B). The width of the "before" region was chosen to match with the width of the stationary site. Δv ($v_{inside} - v_{before}$) for each crossing event was used to determine how the cargo's speed changed (fast, slow or unchanged) when crossing the stationary marker.

RESULTS

Moving TrkA cargos slow down at non-moving TrkA sites in DRG axons

We first examine how the presence of non-moving TrkA organelles affects the transport dynamics of moving TrkA in axons. TrkA is a member of the tyrosine kinase receptors that has a high-affinity binding site for nerve growth factor (NGF) [14]. In DRG neurons, TrkA cargos are separated into two distinct populations with one population transporting in the retrograde direction toward the cell body and the other population moving in the anterograde direction toward the axonal termini (Fig. 1A). On average, the anterograde population moves with a faster speed (v_{ante} = 3.2 ± 1.6 μm/s, n = 433) compared to that of the retrograde population (v_{retro} = 1.6 ± 1.0 μm/s, n = 378). The majority of TrkA cargos move along the axon in a stop-and-go fashion, where active movements are interspersed with intermittent pauses. Nevertheless, a small population of TrkA cargos (about 9% of all TrkA cargos) is found to be stationary at various locations along the axon (Fig. 1A, red arrows).

We quantified how the speed of retrogradely moving TrkA cargos change when crossing the non-moving TrkA sites in the same axon. The distribution of the change in speed, $\Delta v = v_{inside} - v_{before}$, (Fig. 1C) shows that TrkA cargo has a much higher probability of slowing down, i.e. $\Delta v<0$, than speeding up ($\Delta v>0$) when crossing stationary sites (n=351). On the other hand, when moving TrkA cargos cross control sites that are far (at least 10 pixels away) from non-moving TrkA (n=1811), there is about equal probability of the cargo slowing down or speeding up.

To make it easier to visualize the transport behavior of TrkA cargos, we sort the crossing events into three categories: a) slower ($\Delta v<-0.3$ um/s), b) faster ($\Delta v> 0.3$ um/s), and c) unchanged in speed ($|\Delta v| \leq 0.3$ um/s). For retrograde moving TrkA cargos, a significantly larger population slows down than speeds up when crossing non-moving TrkA (61.5 ± 3.0% slower vs. 14.2 ± 1.5% faster, n = 351 events), while no significant difference in the likelihood of TrkA cargos slowing down or speeding up when crossing the control regions (35.4 ± 2.7% slower vs. 35.8 ± 4.0% faster, n=1811 events) (Fig. 1D). Errors are calculated as standard deviation. We also carried out the same measurements for TrkA cargos moving in the anterograde direction, which exhibit very similar behavior – a significantly more antegrogradely moving TrkA cargos slow down when crossing non-moving TrkA (68.6 ± 2.0% slower vs. 16.6±1.8% faster, n = 385 events), while there is no difference of when crossing control sites (37.9 ± 3.1% slow vs. 38.2 ± 3.3% fast, n=2548 events) (Fig. 1E). We note that our kymograph analysis method is a 2D representation of the transport environment inside the axon and thus does not have the resolution in the z-plane (within 1–3 μm depths of the axon). Therefore, it is possible that the analysis also includes some cargos

Author Manuscript Author Manuscript Author Manuscript Author Manuscript

that are not actually cross the non-moving TrkA and hence “dilutes” the slow down effect of the stationary TrkA organelles. However, given this “dilution”, the analysis still shows significant slowdown effect of the non-moving TrkA. This result thus further reinforces the observation that the cargos have a higher tendency to slow down when crossing the stationary TrkA.

Moving TrkA cargos slow down at stationary mitochondrial sites in DRG axons

We next examine the transport behavior of TrkA when crossing stationary mitochondria in DRG neurons by co-transfecting the cells with TrkA-mCherry and Mito-YFP (Fig. 2A–B and Fig. S2). Mitochondria are vital to the health of the neuron by producing ATP, the main energy source for the molecular motors that drive axonal transport [15, 16]. On the other hand, mitochondria are relatively large organelles, with their diameters sometimes match with the slender axonal shafts and therefore may pose as steric hindrance as previously suggested [9, 17].

DRG neurons co-transfected with TrkA-mCherry and Mito-YFP also exhibit robust TrkA transport. The average speed of TrkA cargos in this experiment is 1.7 ± 0.9 μm/s for retrograde transport (n = 496) and 3.2 ± 1.5 μm/s for anterograde transport (n = 622), very similar to neurons singly-transfected with TrkA-mCherry. This result indicates that co-transfecting the neurons with Mito-YFP does not disturb the normal transport behavior of TrkA cargos. Although mitochondria are transporting cargos themselves, in this study we focus on stationary mitochondria, which are defined as mitochondria with average speed less than or equal 0.3 μm/s during the image acquisition period (500 frames).

As TrkA cargos crossed the stationary mitochondria in the axon, we also observed that many cargos clearly slowed down (Fig. 2B, yellow arrows). Similar to the behavioral analysis described in the previous section, we analyzed every encounter between a TrkA cargo and a stationary mitochondrial site using the custom-written Matlab program. As a control, similar analysis was carried out for non-mitochondrial sites using the same sets of movies. The control regions had to be at least 10 pixels away from any mitochondria to exclude any potential interfering effect from neighboring mitochondria. A fixed length of 1.8 μm, the median length of the mitochondrial sites, was chosen for the length of the control sites (Fig. S3).

Quantification of the transport dynamics shows that TrkA cargos have a much higher probability to slow down when crossing mitochondrial sites as compared to crossing the control regions that are absent of mitochondria (Fig. 2C–D). When crossing stationary mitochondrial sites, significantly more retrogradely moving TrkA cargos slow down than speed up (53.8 ± 2.2% vs. 22.9± 3.0%, n = 996). By comparison, retrogradely moving TrkA cargos exhibit equal probability of slowing down or speeding up (36.8 ± 2.7% vs. 37.6 ± 1.9%, n = 1410) when crossing a control region. Similarly, anterograde TrkA cargos slow down for 68.8 ± 3.5% of the time when crossing mitochondrial sites (n = 1258), significantly higher than that of the control regions at 37.9 ± 2.4% (n = 2616). Statistical analysis was conducted using Student t-test, $p<0.001$.

Author Manuscript Author Manuscript Author Manuscript Author Manuscript

If the transport delay is caused by steric hindrance, we expect more delays at larger mitochondria sites. However, we find that the delay of TrkA transport does not depend on the length of the mitochondrial sites (Fig. S4). As shown in Fig. S4, the cargo transport behavior does not change significantly when crossing either small or large mitochondrial sites, where large mitochondria are those with length > 1.8 μm (n = 332, average length 2.6 ± 0.7 μm), and small mitochondria are those with length ≤ 1.8 μm (n = 573, average length 1.5 ± 0.4 μm). For retrograde cargos, 54.9 ± 5.0% of the population slows down at small mitochondrial sites (n = 568), whereas 54.1 ± 2.3% of them slows down at large mitochondrial sites (n = 428) (Fig. S4A). The slow down rate of anterograde TrkA cargos at small mitochondrial sites (70.5 ± 2.1%, n = 646) is also comparable to that of large mitochondrial sites (64.7 ± 1.8%, n = 612) (Fig. S4B).

TrkA cargos pause longer and more frequently at mitochondrial sites

As seen in Fig. 2B, some TrkA cargos not only slow down at mitochondrial site, but actually pause for some period of time before resuming motion to cross the mitochondrial region. Pauses are interesting features of cargo axonal transport as they could be the indication of a cargo struggling to cross an obstacle on the microtubule track [7]. Therefore, we next examine the pausing behavior of TrkA cargos at mitochondrial sites. For this analysis, each TrkA trajectory was parsed into a series of connected straight-line segments using linear regression (Fig. S5). A pause is defined as a segment with a velocity less than or equal to 0.3 μm/s. The pauses in all TrkA trajectories are separated into two groups: pauses that occur at mitochondrial sites and pauses that occur at non-mitochondrial sites. Pausing frequency of retrograde cargo at the mitochondrial site is calculated to be 0.24 ± 0.04 pause/μm, which is significantly higher than the pausing frequency at locations without stationary mitochondria (0.13 ± 0.02 pause/μm). For anterograde transport, the pausing frequency at mitochondria site is 0.16 ± 0.04 pause/μm, which is twice the pausing frequency at regions absent of mitochondria (0.08 ± 0.01 pause/μm). Errors show SEM, n = 7 independent cultures.

Not only TrkA cargos pause more frequently at mitochondrial site compare to region not associated with mitochondria, the cargos also tend to pause longer at mitochondrial sites (Fig.2E–F). For pauses in the retrograde direction, the average duration is 5.1 ± 0.3s at the mitochondrial sites (n = 418), which is significantly longer than that of pauses not associated with mitochondria (3.9 ± 0.2s, n = 957). Similarly, in anterograde cargos, the average pause duration at mitochondrial site (7.3 ± 0.5s, n = 274) is also longer than the average duration of pauses not associated with mitochondria (6.8 ± 0.3s, n = 605). The average pause duration observed at the mitochondrial sites is comparable to the pause duration reported for cargo's interaction with local axonal structures (4.7–7.5s) [7, 8].

Lysosomes and TrkB also slow down at mitochondrial sites

There are earlier studies reporting that NGF signaling can facilitate the docking of mitochondria in DRG neurons [18, 19]. Since NGF binds preferentially to TrkA receptors, it is possible that the transport delay effect of mitochondria is only specific to TrkA cargos due to a particular signaling interaction in DRG neurons. To investigate whether the transport delay caused by stationary mitochondria is specific to TrkA cargos, we carried out the same speed analysis in the axonal transport of lysosomes in DRG neurons (Fig. 3A–C). Similar to

Author Manuscript Author Manuscript Author Manuscript Author Manuscript

TrkA transport, lysosomes have a significantly high tendency to slow down when crossing mitochondrial sites (Fig. 3A). For lysosomes moving in the retrograde direction, 52.4 ± 1.0% of the population slows down at mitochondrial sites (n=540), compared to 36.4 ± 1.8% at non-mitochondrial sites (n=769). In the anterograde direction, 57.0 ± 2.1% of the cargos decreases the speed when crossing mitochondrial sites (n=454), compared to 41.8 ± 0.9% at non-mitochondrial sites (n=697).

Next, we look into the transport behavior of TrkB-containing cargos in hippocampal neurons to ensure that the observed mitochondrial delay effect is not specific to DRG neurons (Fig. 3D–F). TrkB is a homolog of TrkA receptor in hippocampal neurons. We again observe the same trend where TrkB has significantly high propensity to slow down the transport speed at mitochondrial sites. For retrograde TrkB transport, 57.1 ± 1.5% of the population slows down at mitochondrial sites (n=184), compared to 41.2 ± 2.3% at non-mitochondrial sites (n=359). For TrkB travelling in the anterograde direction, 55.2 ± 1.7% of the population slows down at mitochondrial sites (n=154), compared to 41.0 ± 0.8% at non-mitochondrial sites (n=329).

DISCUSSION AND CONCLUSIONS

In this study, we have examined the potential effect of stationary axonal structures to the transport of cargos in neurons using dual-color fluorescent imaging. Transport behavior of TrkA in DRG neurons reveals that cargos tend to significantly slow down, or even pause for some period of time when crossing stationary organelles along the axon such as mitochondria and other stationary TrkA cargos. This behavior is observed for both anterograde and retrograde directions. Our experimental results also reveal that cargos tend to pause longer, and more frequently at mitochondrial sites compared to regions that are not associated with mitochondria. Similar results are observed in lysosomal axonal transport in DRG neurons and TrkB transport in hippocampal neurons.

The presence of stationary organelles and the slowing down of axonal cargos could be either causative or correlative. On the one hand, the bulky stationary structures may directly cause the delay of other axonal cargos. One can view the inside of an axon as a crowded traffic highway, where cargos moving in opposite directions must share the same set of traffic lanes, i.e. microtubules. Over a long distance, the cargo has to maneuver through a dense axoplasm where it inevitably crosses other trafficking cargos and structures along the microtubules. Therefore, stationary organelles situated along the axon can slow down the axonal transport of other cargos by posing as steric hindrance. This hypothesis is consistent with previous report showing that mitochondrial swelling induced by drugs could significantly impair the axonal transport of cargos in neurons [9, 10]. We note that the effect observed in our study is statistically significant but rather mild in a healthy neuron, where the axonal structures do not abrogate the movement but only slightly delay the transport.

On the other hand, it is possible that the observed effect is not directly caused by steric hindrance. Stationary organelles in axons may be anchored locally because of local microtubule defects or other local features, which also causes delay in the cargo transport. This scenario is supported by our results showing that stationary TrkA organelles cause

Author Manuscript Author Manuscript Author Manuscript Author Manuscript

similar transport delay than stationary mitochondria despite that the size of TrkA organelle is much smaller than that of mitochondria. This scenario is also supported by our results that the delay of moving cargos does not depend on the size of the mitochondria. However, we acknowledge that the measured mitochondrial length does not fully reflect the true mitochondrial size. The fluorescent kymograph is only a 2-dimensional representation of the mitochondria, which does not provide information about the width of the mitochondria. Furthermore, it is possible that some mitochondrial sites could be aggregates of many mitochondria stuck in one place, which is difficult to discern using the kymographs. Further studies are needed to understand the mechanisms of how stationary axonal organelles causes transport delays.

Supplementary Material

Refer to Web version on PubMed Central for supplementary material.

ACKNOWLEDGEMENTS

We thank Ari Helenius (ETH Zurich, Switzerland) for the LAMP1-mCherry plasmid; and Chengbiao Wu (University of California, San Diego) for the TrkB-mCherry plasmid. The authors are grateful for financial support from the NIH New Innovator Award (DP2NS082125), the Searle Scholar Award, and the Packard Science and Engineering Fellowship. D.L.C. is supported by the National Science Foundation Graduate Fellowship.

REFERENCES

1. Grafstein, B. Comprehensive Physiology. John Wiley & Sons, Inc; 2011. Axonal Transport: The Intracellular Traffic of the Neuron.
2. De Vos, KJ.; Grierson, AJ.; Ackerley, S.; Miller, CCJ. Annual Review of Neuroscience. Vol. 31. Palo Alto: Annual Reviews; 2008. Role of axonal transport in neurodegenerative diseases; p. 151-173.
3. Stokin GB, Lillo C, Falzone TL, Brusch RG, Rockenstein E, Mount SL, Raman R, Davies P, Masliah E, Williams DS, Goldstein LSB. Axonopathy and transport deficits early in the pathogenesis of Alzheimer's disease. Science. 2005; 307:1282–1288. [PubMed: 15731448]
4. Bilsland LG, Sahai E, Kelly G, Golding M, Greensmith L, Schiavo G. Deficits in axonal transport precede ALS symptoms in vivo. Proc. Natl. Acad. Sci. U. S. A. 2010; 107:20523–20528. [PubMed: 21059924]
5. Chevalier-Larsen E, Holzbaur ELF. Axonal transport and neurodegenerative disease. Biochimica Et Biophysica Acta-Molecular Basis of Disease. 2006; 1762:1094–1108.
6. Hafezparast M, Klocke R, Ruhrberg C, Marquardt A, Ahmad-Annuar A, Bowen S, Lalli G, Witherden AS, Hummerich H, Nicholson S, Morgan PJ, Oozageer R, Priestley JV, Averill S, King VR, Ball S, Peters J, Toda T, Yamamoto A, Hiraoka Y, Augustin M, Korthaus D, Wattler S, Wabnitz P, Dickneite C, Lampel S, Boehme F, Peraus G, Popp A, Rudelius M, Schlegel J, Fuchs H, de Angelis MH, Schiavo G, Shima DT, Russ AP, Stumm G, Martin JE, Fisher EMC. Mutations in dynein link motor neuron degeneration to defects in retrograde transport. Science. 2003; 300:808–812. [PubMed: 12730604]
7. Balint S, Verdeny Vilanova I, Sandoval Alvarez A, Lakadamyali M. Correlative live-cell and super resolution microscopy reveals cargo transport dynamics at microtubule intersections. Proceedings of the National Academy of Sciences of the United States of America. 2013; 110:3375–3380. [PubMed: 23401534]
8. Zajac AL, Goldman YE, Holzbaur ELF, Ostap EM. Local Cytoskeletal and Organelle Interactions Impact Molecular-Motor-Driven Early Endosomal Trafficking. Current Biology. 2013; 23:1173–1180. [PubMed: 23770188]

Author Manuscript Author Manuscript Author Manuscript Author Manuscript

9. Safiulina D, Veksler V, Zharkovsky A, Kaasik A. Loss of mitochondrial membrane potential is associated with increase in mitochondrial volume: Physiological role in neurones. J Cell Physiol. 2006; 206:347–353. [PubMed: 16110491]
10. Kaasik A, Safiulina D, Choubey V, Kuum M, Zharkovsky A, Veksler V. Mitochondrial swelling impairs the transport of organelles in cerebellar granule neurons. J Biol Chem. 2007; 282:32821–32826. [PubMed: 17785462]
11. Chan JR, Rodriguez-Waitkus PM, Ng BK, Liang P, Glaser M. Progesterone synthesized by Schwann cells during myelin formation regulates neuronal gene expression. Mol. Biol. Cell. 2000; 11:2283–2295. [PubMed: 10888668]
12. Zhang K, Osakada Y, Vrljic M, Chen LA, Mudrakola HV, Cui BX. Single-molecule imaging of NGF axonal transport in microfluidic devices. Lab Chip. 2010; 10:2566–2573. [PubMed: 20623041]
13. Zhang K, Osakada Y, Xie WJ, Cui BX. Automated Image Analysis for Tracking Cargo Transport in Axons. Microsc. Res. Tech. 2011; 74:605–613. [PubMed: 20945466]
14. Wiesmann C, Ultsch MH, Bass SH, de Vos AM. Crystal structure of nerve growth factor in complex with the ligand-binding domain of the TrkA receptor. Nature. 1999; 401:184–188. [PubMed: 10490030]
15. Pickrell AM, Moraes CT. What role does mitochondrial stress play in neurodegenerative diseases? Methods Mol Biol. 2010; 648:63–78. [PubMed: 20700705]
16. Mahad D, Lassmann H, Turnbull D. Review: Mitochondria and disease progression in multiple sclerosis. Neuropathology and Applied Neurobiology. 2008; 34:577–589. [PubMed: 19076696]
17. Shepherd GMG, Harris KM. Three-dimensional structure and composition of CA3 ->CA1 axons in rat hippocampal slices: Implications for presynaptic connectivity and compartmentalization. J. Neurosci. 1998; 18:8300–8310. [PubMed: 9763474]
18. Chada SR, Hollenbeck PJ. Mitochondrial movement and positioning in axons: the role of growth factor signaling. Journal of Experimental Biology. 2003; 206:1985–1992. [PubMed: 12756280]
19. Chada SR, Hollenbeck PJ. Nerve growth factor signaling regulates motility and docking of axonal mitochondria. Curr. Biol. 2004; 14:1272–1276. [PubMed: 15268858]

Author Manuscript Author Manuscript Author Manuscript Author Manuscript

Highlights

- Dual-color imaging technique was used to observe the axonal transport dynamics between axonal cargos and stationary organelles in dorsal root ganglion neurons.
- Axonal cargos tend to transiently slow down, or pause within the vicinity of the stationary organelles, suggesting that stationary organelles can pose as mild steric hindrance to axonal transport.
- Further investigations are needed to understand the causative or correlative relationship between stationary organelles and transport delays of axonal cargoes.

Author Manuscript
Author Manuscript
Author Manuscript
Author Manuscript

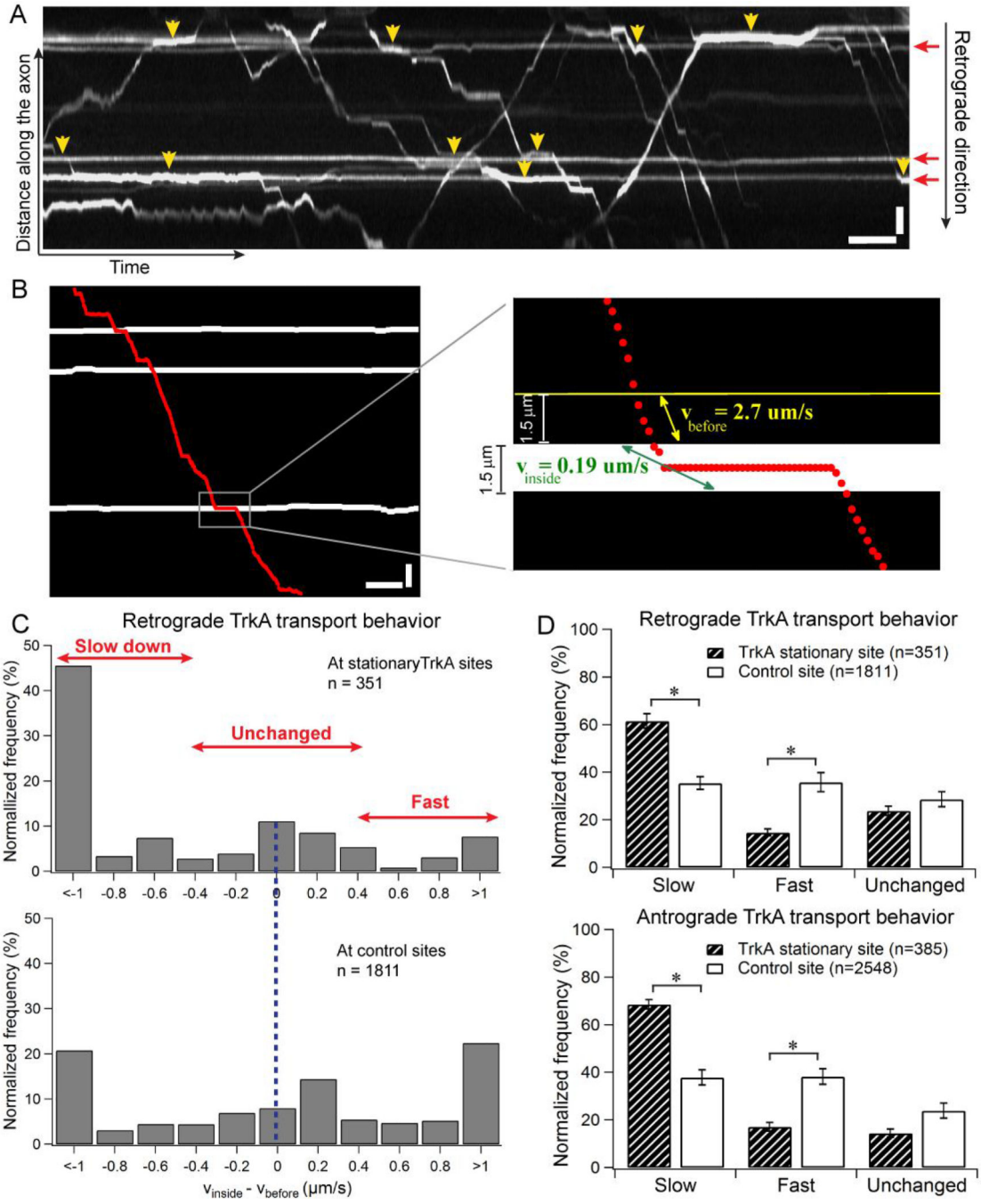

Figure 1.

Moving TrkA cargos slow down when crossing stationary TrkA markers in DRG axons. (A) Kymograph of TrkA trajectories in DRG neurons transfected with TrkA-mCherry. Horizontal lines (red arrows) indicate the stationary TrkA in the axon. Yellow arrowheads show the regions where the moving TrkA cargos clearly slow down when crossing the stationary TrkA. (B) The process of quantifying TrkA transport behavior when crossing stationary markers. The trajectory of a retrograde TrkA cargo (red dots) is overlapped onto the positions of the stationary TrkA (white horizontal lines) in the same axon. Inset shows

Author Manuscript Author Manuscript Author Manuscript Author Manuscript

enlarged image of a crossing event (gray rectangle in the original kymograph), where the speed of the cargo right before the stationary TrkA region (v_{before}, yellow) is compared to the speed of the cargo inside the stationary TrkA region (v_{inside}, green). (C) Comparison of the distribution of Δv ($v_{before}-v_{inside}$) for retrogradely moving TrkA cargos when crossing stationary TrkA sites (n=351) vs. when crossing control sites that are absent of stationary TrkA (n=1811). (D) TrkA transport behavior when crossing stationary TrkA markers is categorized into three groups – slow, fast and unchanged based on Δv ($v_{before}-v_{inside}$) values. Data were cumulated from 7 independent experiments. The cargo behavior is normalized to the total number of crossing events. Bootstrapping (10 sets of 300 randomly selected events) was performed to calculate the standard deviation. Error bars represents standard deviation. Statistical significance was assessed using Student's t-test, $p<0.001$. Horizontal bar, 5s. Vertical bar, 5 μm.

Author Manuscript
Author Manuscript
Author Manuscript
Author Manuscript

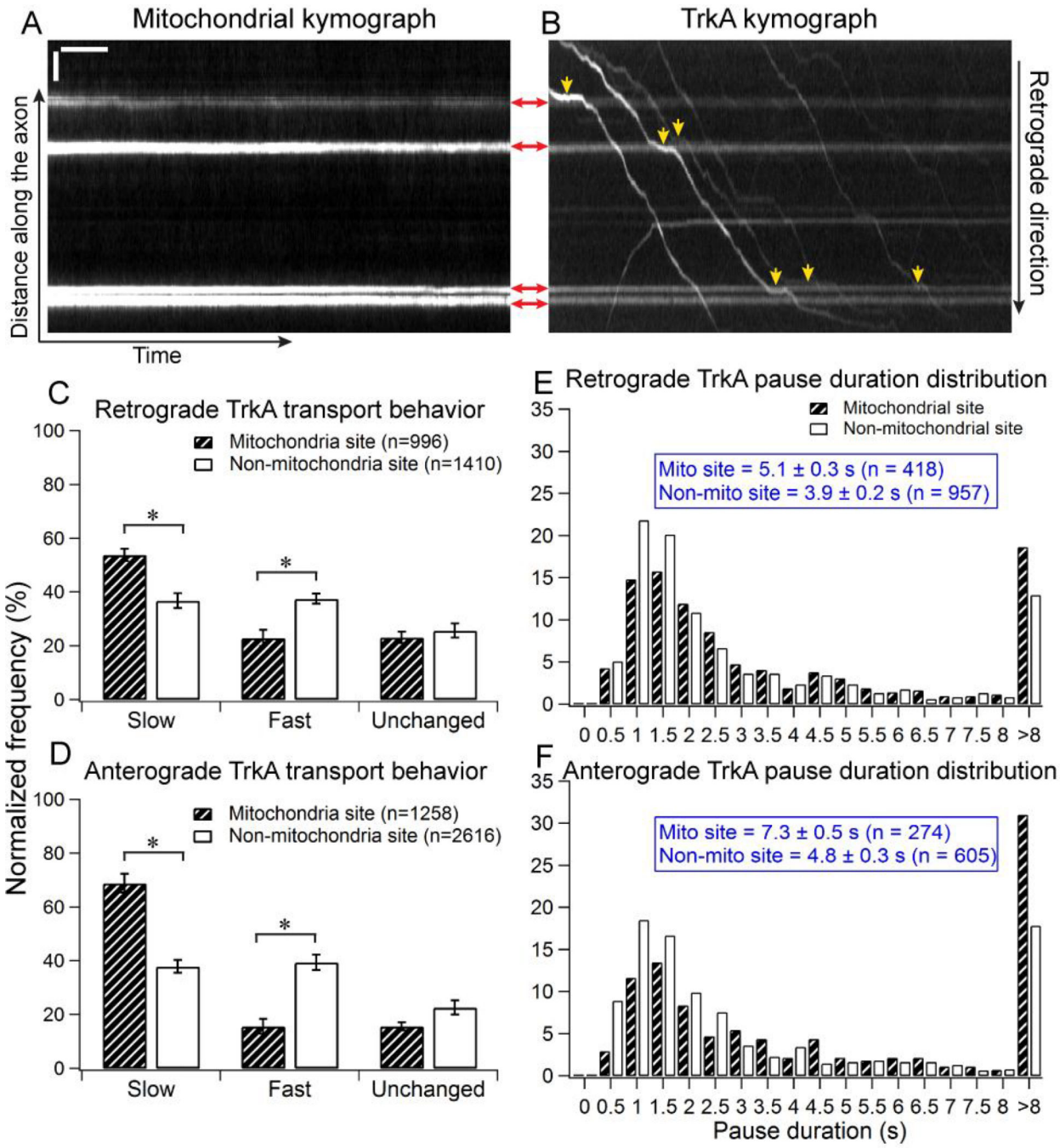

Figure 2.

Moving TrkA cargos slow down when crossing stationary mitochondria in DRG axons. DRG neurons are co-transfected with TrkA-mCherry and Mito-YFP. (A) A representative mitochondrial kymograph. Horizontal lines indicate the stationary mitochondria in the axon. (B) The kymograph of TrkA cargos in the same axon. Shadows of the four mitochondria in the axon can also be seen on TrkA kymograph. Red arrows show the positions of mitochondriain both the mitochondrial and TrkA kymographs. Yellow arrowheads indicate the regions where TrkA cargos clearly slow down when crossing the stationary

Author Manuscript Author Manuscript Author Manuscript Author Manuscript

mitochondria in the axon. Horizontal bar, 5s.Vertical bar, 5μm. (C–D) Quantification of TrkA transport behavior in the retrograde direction (C) and the anterograde direction (D). Data were cumulated from 7 independent experiments. Bootstrapping (10 sets of 300 randomly selected events) was performed to calculate the standard deviation. Error bars represents standard deviation. Statistical significance was assessed using Student's t-test, $p<0.001$. (E–F) The distribution of pause duration for TrkA cargos at mitochondrial sites compared to control sites that are not associated with mitochondria. Data were cumulated from 7 independent experiments.

Author Manuscript Author Manuscript Author Manuscript Author Manuscript

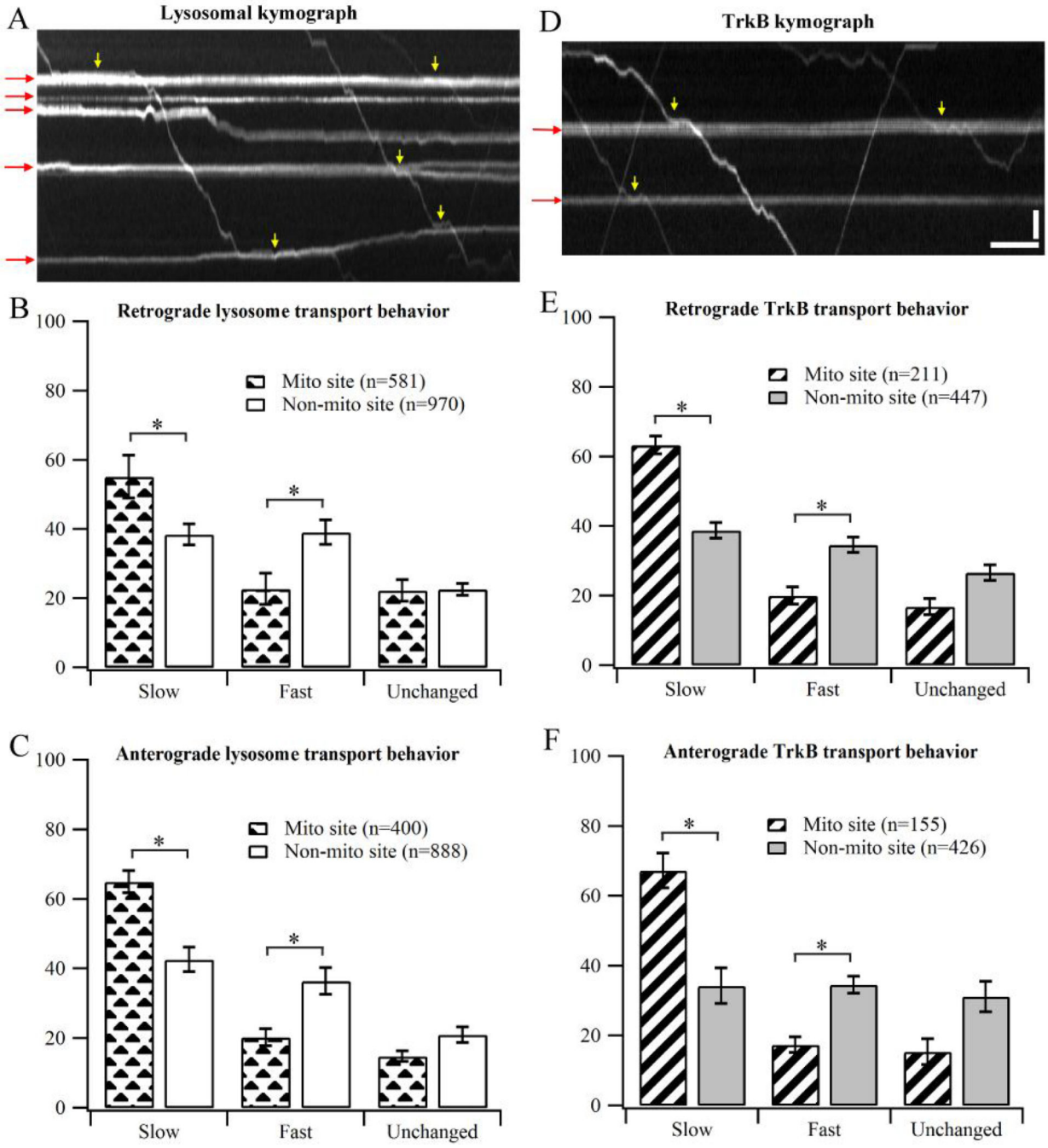

Figure 3.

Transport behavior of lysosomes and TrkB when crossing stationary mitochondria. (A) Representative kymograph showing transport behavior of lysosomes in DRG neurons. Red arrows indicate stationary mitochondrial traces in the kymograph. Yellow arrows show the regions where the cargos clearly slow down at mitochondrial sites. (B–C) Transport behavior of lysosomes in DRG neurons. Data were cumulated from 3 independent cultures. (D) Representative kymograph showing transport behavior of TrkB in hippocampal neurons. (E–F) Behavior of TrkB transport in hippocampal neurons. Data were cumulated from 4

independent cultures. Error bars show standard deviation. Bootstrapping (10 sets of 200 randomly selected events) was performed to calculate the standard deviation. Statistical significance was assessed using Student's t-test, $p<0.001$. Horizontal bar, 5s.Vertical bar, 5 μm.

Author Manuscript Author Manuscript Author Manuscript Author Manuscript